PRAMANA
— journal of
physics

Vol. 63, No. 3
September 2004
pp. 529–541

Photon mass attenuation coefficients, effective atomic numbers and electron densities of some thermoluminescent dosimetric compounds

SHIVALINGE GOWDA, S KRISHNAVENI, T YASHODA, T K UMESH* and RAMAKRISHNA GOWDA
Department of Studies in Physics, University of Mysore, Mysore 570 006, India
*Author for correspondence
E-mail: tku@uomphysics.net; tku1@yahoo.com

MS received 17 June 2003; revised 15 April 2004; accepted 15 June 2004

Abstract. Photon mass attenuation coefficients of some thermoluminescent dosimetric (TLD) compounds, such as LiF, $CaCO_3$, $CaSO_4$, $CaSO_4{\cdot}2H_2O$, $SrSO_4$, $CdSO_4$, $BaSO_4$, $C_4H_6BaO_4$ and $3CdSO_4{\cdot}8H_2O$ were determined at 279.2, 320.07, 514.0, 661.6, 1115.5, 1173.2 and 1332.5 keV in a well-collimated narrow beam good geometry set-up using a high resolution, hyper pure germanium detector. The attenuation coefficient data were then used to compute the effective atomic number and the electron density of TLD compounds. The interpolation of total attenuation cross-sections of photons of energy E in elements of atomic number Z was performed using the logarithmic regression analysis of the data measured by the authors and reported earlier. The best-fit coefficients so obtained in the photon energy range of 279.2 to 320.07 keV, 514.0 to 661.6 keV and 1115.5 to 1332.5 keV by a piece-wise interpolation method were then used to find the effective atomic number and electron density of the compounds. These values are found to be in agreement with other available published values.

Keywords. Thermoluminescent dosimetric compounds; mass attenuation coefficients; effective atomic number and electron density.

PACS Nos 31.70.-f; 32.10.-f; 32.80.-t; 32.90.+a

1. Introduction

The mass attenuation coefficient, the effective atomic number and the electron density are basic quantities required in determining the penetration of X-ray and photons in matter. The measurement of attenuation coefficients of photons in biological and other materials is of significant interest in industrial, biological, agricultural and medical applications. Accurate values of photon mass attenuation coefficients are needed to establish the regions of validity of theory-based parametrization, in addition to providing essential data in such diverse fields such as tomography, γ-ray fluorescence studies and radiation biophysics. The mass attenuation coefficients are

also widely used in the calculation of photon penetration and energy deposition in biological, shielding and other dosimetric materials [1–9]. In order to select the most suitable material for radiation dosimetry, the characteristics of the various materials must be known [10,11].

The scattering and absorption of γ-radiations are related to the density and effective atomic number of the material. The effective atomic number and the electron density of a composite material are very useful parameters in the dosimetric calculation of radiation dose in radiotherapy [12] and also in medical imaging, where the cross-sectional anatomy is generated by computer-aided tomography (CAT). These parameters have physical meaning and their numerical value allows many characteristics of a material to be visualized. Several commercially available thermoluminescent and photoluminescent materials are used as radiation detectors in biological and industrial dosimetry of ionizing radiations.

Hine [13] pointed out that, in photon interaction in the composite materials, the atomic number cannot be represented uniquely by a single number across the entire energy region, as in the case of pure elements. This number for composite materials is called the effective atomic number and it varies with the energy. Following Hine's suggestions, many attempts have been made to determine effective atomic number (Z_{eff}) for partial and total interactions in alloys and compounds [6,14–18]. Some empirically deduced formulae have also been reported in literature [19] but their validity is limited to the experimental conditions used in that work. Tabulations of photon mass attenuation coefficients and interaction cross-sections have been published for several elements and composite materials, which are of dosimetric and radiological interest [20]. Berger and Hubbell [21] have developed a computer program, XCOM, which calculates photon cross-sections and attenuation coefficients for pure elements and mixtures in the energy range of 1 keV to 100 GeV.

In this paper, we report accurate measured values of total attenuation coefficients (cross-sections), effective atomic numbers and the electron densities of TLD compounds at the energies 279.2, 320.07, 514.0, 661.6, 1115.5, 1173.2 and 1332.5 keV obtained by experiments. These attenuation coefficient values were used to determine the effective atomic number and electron density of several TLD compounds as indicated earlier. The E- and Z-wise interpolation of total attenuation cross-sections of the elements was performed using the logarithmic regression analysis of the data measured by the authors and reported earlier [22–25]. The best-fit coefficients so obtained in the energy range of 279.2 to 320.07 keV, 514.0 to 661.6 keV and 1115.5 to 1332.5 keV by a piece-wise interpolation method, were then used to find the effective atomic number and electron density of the compounds.

2. Theory

As the materials are composed of various elements, it is assumed that the contribution of each element of the compound to total photon interaction is additive, yielding the well-known 'mixture rule' [26] that represents the total mass attenuation coefficient $(\mu/\rho)_c$ of any compound as the sum of the appropriately weighted proportions of the individual atoms. Thus,

$$\left(\frac{\mu}{\rho}\right)_c = \sum_i W_i \left(\frac{\mu}{\rho}\right)_i, \tag{1}$$

where $(\mu/\rho)_c$ is the photon mass attenuation coefficient for the compound, $(\mu/\rho)_i$ is the photon mass attenuation coefficient for the individual elements in the compound, and W_i is the fractional weight of the elements in the compound. For any compound, a quantity called the effective atomic cross-section, $\sigma_{\rm a}$, is defined according to [2]. Clearly, in calculating $\sigma_{\rm a}$, averaging is carried out over atoms of all the elements in the compound. Thus, we have,

$$\sigma_{\rm a} = \frac{(\mu/\rho)_c}{N_{\rm A} \sum_i \frac{W_i}{A_i}}, \tag{2}$$

where $N_{\rm A}$ is the Avogadro's number and A_i is the atomic weight of the constituent element.

Similarly, the average electronic cross-section, $\sigma_{\rm el}$, is given by

$$\sigma_{\rm el} = \frac{1}{N_{\rm A}} \sum_i f_i \frac{A_i}{Z_i} \left(\frac{\mu}{\rho}\right)_i, \tag{3}$$

where $f_i = (n_i / \sum_j n_j)$ and Z_i are the fractional abundance and atomic number respectively of the constituent element. Here, n_i is the total number of atoms of the constituent element and $\sum_j n_j$ are the total number of atoms of all types present in the compound as per its chemical formula. The effective atomic number, $Z_{\rm eff}$, can now be written as

$$Z_{\rm eff} = \frac{\sigma_{\rm a}}{\sigma_{\rm el}}. \tag{4}$$

Other expressions for the effective atomic numbers are found in [6,12,14,16]. The effective electron number or density, $N_{\rm el}$ (number of electrons per unit mass) can be found from

$$N_{\rm el} = \frac{(\mu/\rho)_c}{\sigma_{\rm el}}. \tag{5}$$

3. Experimental set-up and measurements

The radioactive sources ^{203}Hg, ^{51}Cr, ^{85}Sr, ^{137}Cs, ^{65}Zn and ^{60}Co were used in the present investigation. Each γ-ray of energy 279.2, 320.07, 514.0, 661.6, 1115.5, 1173.2, 1332.5 keV emitted by the above radioactive isotopes were collimated and detected by an ORTEC model 23210 'Gamma-X' high-purity germanium detector having energy resolution of 2.5 keV at 1332.5 keV. The signals from the detector were suitably amplified and analysed with 8K-multichannel analyser.

In the photon transmission experiment, the photon spectra were recorded for each source by placing the empty container and the container filled with the sample

Table 1. Experimentally measured values of photon mass attenuation coefficients $(\mu/\rho)_c$ for some TLD compounds in cm^2/g.

	Photon energy (keV)						
Compound	279.2	320.07	514.0	661.6	1115.5	1173.2	1332.5
LiF	0.1008 ± 0.0029	0.0950 ± 0.0027	0.0801 ± 0.0023	0.0711 ± 0.0021	0.0555 ± 0.0017	0.0537 ± 0.0015	0.0506 ± 0.0014
	(0.1017)	(0.0963)	(0.0798)	(0.0715)	(0.0558)	(0.0544)	(0.0510)
$CaSO_4{\cdot}2H_2O$	0.1129 ± 0.0034	0.1069 ± 0.0030	0.0884 ± 0.0025	0.0833 ± 0.0024	0.0619 ± 0.0019	0.0605 ± 0.0018	0.0562 ± 0.0016
				0.0790 ± 0.002*			
	(0.1142)	(0.1076)	(0.0886)	(0.0792)	(0.0618)	(0.0602)	(0.0564)
$CaCO_3$	0.1113 ± 0.0032	0.1043 ± 0.0031	0.0859 ± 0.0026	0.0772 ± 0.0022	0.0605 ± 0.0018	0.0591 ± 0.0017	0.0554 ± 0.0017
	(0.1121)	(0.1054)	(0.0867)	(0.0775)	(0.0604)	(0.0589)	(0.0552)
$C_4H_6BaO_4$	0.1649 ± 0.0049	0.1405 ± 0.0041	0.0928 ± 0.0027	0.0791 ± 0.0024	0.0583 ± 0.0017	0.0571 ± 0.0016	0.0529 ± 0.0015
				0.0810 ± 0.0002*			
	(0.1677)	(0.1411)	(0.0938)	(0.0793)	(0.0584)	(0.0568)	(0.0530)
$3CdSO_4{\cdot}8H_2O$	0.1383 ± 0.0040	0.1228 ± 0.0036	0.0890 ± 0.0026	0.0779 ± 0.0023	0.0591 ± 0.0017	0.0581 ± 0.0017	0.0537 ± 0.0016
				0.0750 ± 0.002*			
	(0.1403)	(0.1234)	(0.0900)	(0.0781)	(0.0591)	(0.0575)	(0.0538)
$CaSO_4$	0.1121 ± 0.0033	0.1047 ± 0.0031	0.0862 ± 0.0025	0.0777 ± 0.0022	0.0605 ± 0.0018	0.0591 ± 0.0018	0.0553 ± 0.0017
	(0.1122)	(0.1055)	(0.0867)	(0.0775)	(0.0604)	(0.0589)	(0.0552)
$SrSO_4$	0.1212 ± 0.0036	0.1096 ± 0.0033	0.0846 ± 0.0024	0.0741 ± 0.0021	0.0573 ± 0.0017	0.0561 ± 0.0017	0.0525 ± 0.0015
				0.0770 ± 0.002*			
	(0.1219)	(0.1103)	(0.0848)	(0.0746)	(0.0572)	(0.0558)	(0.0522)
$CdSO_4$	0.1425 ± 0.0042	0.1245 ± 0.0037	0.0872 ± 0.0025	0.0760 ± 0.0022	0.0572 ± 0.0017	0.0563 ± 0.0017	0.0524 ± 0.0016
	(0.1446)	(0.1253)	(0.0886)	(0.0763)	(0.0573)	(0.0557)	(0.0521)
$BaSO_4$	0.1676 ± 0.0050	0.1417 ± 0.0042	0.0900 ± 0.0026	0.0776 ± 0.0022	0.0564 ± 0.0017	0.0554 ± 0.0017	0.0516 ± 0.0015
				0.0770 ± 0.002*			
	(0.1708)	(0.1424)	(0.0924)	(0.0775)	(0.0566)	(0.0551)	(0.0514)

XCOM values in bracket and values from [10] (at 661.6 keV, marked by *) are shown for comparison.

TLD compound alternately in the path of the incident beam. This procedure was repeated at least ten times for each sample. The intensities of the incident and transmitted photons were determined by choosing the counting time such that, at least 10^5–10^6 counts were recorded under the photo peak. Thus the statistical uncertainty was kept below 0.3%.

The compounds under investigation were confined in cylindrical plastic containers of inner diameter 1.5 cm. The inner diameter of each container was determined separately with the help of a travelling microscope. It was found that the attenuation of the photon beam by the material of the empty containers was negligible. Each sample thus prepared was weighed in a digital balance capable of weighing up to a fraction of a milligram. The weighing was repeated a number of times to obtain consistent values of the mass. The mean of this set of values was taken to be the mass of the sample. By using the inner diameter of the container and the mean value of the mass of the sample, the mass per unit area was determined for each sample. The thickness of the sample was chosen such that the product $\mu t < 0.4$ for all the samples to minimize the effects due to multiple scattering.

From the measured values of unattenuated photon intensity I_0 (with empty plastic container) and attenuated photon intensity I (with sample), the mass attenuation coefficients $(\mu/\rho)_c$ of all TLD compounds were calculated by using the relation

$$\left(\frac{\mu}{\rho}\right)_c = \left(\frac{\ln(I_0/I)}{\rho t}\right), \tag{6}$$

where ρt = mass per unit area in g/cm^2. The values of the mass attenuation coefficients so obtained for all compounds are listed in table 1 along with the XCOM values obtained at all photon energies of current interest shown in brackets [21] and other experimental values available at 661.6 keV [10]. An agreement of less than $\pm 3\%$ between the present and the published values [10] was observed on comparison at photon energy of 661.6 keV from ^{137}Cs for most of the TLD compounds.

4. Results and discussion

Apart from multiple scattering effects and counting statistics, there are several other possible sources of error in the present method. These are due to (a) small-angle scattering contributions, (b) sample impurity, (c) non-uniformity of the sample, (d) photon build-up effects, (e) dead time of the counting instrument and (f) pulse pile up effects. These were evaluated as follows:

(a) *Small-angle scattering*: By keeping a distance of 50 cm from the detector to the source, the maximum angle of scattering from the source to the detector was brought down to 30 min. According to theoretical estimates [27], the contribution of coherent as well as incoherent scattering at such angles in the measured cross-sections at intermediate energies is negligible. Hence no small-angle corrections were applied to the measured data.

(b) *Sample impurity*: The error due to sample impurity can be high only when a large percentage of high-Z impurities is present in the sample. In all the compounds used in the present study, the content of high-Z impurities was <0.005%. Hence, sample impurity corrections were not applied to the measured data.

Table 2. Effective atomic cross-sections, σ_a (b/atom) of some TLD compounds.

Compound	Photon energy (keV)						
	279.2	320.07	514.0	661.6	1115.5	1173.2	1332.5
LiF	2.170 ± 0.064	2.045 ± 0.061	1.720 ± 0.051	1.530 ± 0.045	1.195 ± 0.036	1.155 ± 0.034	1.090 ± 0.032
$CaSO_4{\cdot}2H_2O$	2.689 ± 0.080	2.548 ± 0.075	2.105 ± 0.063	1.985 ± 0.060	1.475 ± 0.044	1.441 ± 0.042	1.340 ± 0.039
$CaCO_3$	3.700 ± 0.109	3.466 ± 0.103	2.856 ± 0.085	2.566 ± 0.076	2.012 ± 0.060	1.964 ± 0.059	1.844 ± 0.054
$C_4H_6BaO_4$	4.662 ± 0.140	3.972 ± 0.118	2.623 ± 0.078	2.237 ± 0.066	1.648 ± 0.048	1.616 ± 0.048	1.496 ± 0.045
$3CdSO_4{\cdot}8H_2O$	4.208 ± 0.125	3.736 ± 0.115	2.709 ± 0.080	2.371 ± 0.069	1.797 ± 0.053	1.768 ± 0.052	1.635 ± 0.049
$CaSO_4$	4.224 ± 0.127	3.945 ± 0.117	3.247 ± 0.096	2.926 ± 0.085	2.280 ± 0.067	2.225 ± 0.067	2.086 ± 0.063
$SrSO_4$	6.160 ± 0.184	5.568 ± 0.165	4.300 ± 0.128	3.765 ± 0.112	2.913 ± 0.087	2.851 ± 0.086	2.668 ± 0.080
$CdSO_4$	8.218 ± 0.245	7.183 ± 0.215	5.028 ± 0.151	4.382 ± 0.130	3.300 ± 0.099	3.250 ± 0.095	3.023 ± 0.091
$BaSO_4$	10.827 ± 0.322	9.150 ± 0.273	5.813 ± 0.173	5.015 ± 0.149	3.652 ± 0.108	3.578 ± 0.106	3.338 ± 0.99

Table 3. Best-fit coefficient values of $\ln A_1, \ln A_2, B_1$ and B_2.

Photon energy range (keV)	Range of atomic number (Z)	Intercept $\ln A_1$	Slope B_1	Intercept $\ln A_2$	Slope B_2
279.2–320.07	3–8	2.23659	0.28653	−0.57359	0.12472
	8–13	−2.64248	2.72379	0.26684	−0.29537
	13–28	−2.79248	2.60672	0.23994	−0.25253
514.0–661.6	3–8	5.95289	−1.40309	−1.1367	0.37561
	8–13	1.83758	0.73173	−0.54863	0.06533
	13–28	−2.44084	2.19505	−0.00367	−0.12231
1115.5–1332.5	3–13	2.00451	0.98356	−0.51726	0.00362
	13–28	1.90538	1.05616	−0.51735	−0.00146

(c) *Non-uniformity of the sample*: The non-uniformity of the sample material introduces a fractional error of about half the root mean square deviation in mass per unit area. The error $\Delta(\mu/\rho)$ in the mass attenuation coefficient due to absorber's non-uniformity was calculated using the relation [28]

$$\Delta\left(\frac{\mu}{\rho}\right) = \frac{1-(\rho/a\mu)\sinh(a\mu/\rho)}{\ln \bar{R}}, \tag{7}$$

where $\bar{R}$ is the mean transmission ratio for obtaining a value of (μ/ρ), a is the maximum deviation of absorber thickness, and ρ is the density of the absorber. Since the uncertainty in the mass per unit area is <0.05% in the present investigation, the error due to non-uniformity of the sample calculated using eq. (7) is <0.05% for all energies of interest.

(d) *Photon build-up effects*: Any sample kept in the path of the photon beam will present an effective mean free path for its interaction. In a good geometry of a narrow beam, most of the incident photons are absorbed and a few are scattered. The absorbed photons can release K-, L-, or M-shell electrons by the photoeffect in the sample followed by bremsstrahlung. The scattered photons can cause multiple scattering, resulting in several energy-degraded photons, which can contribute to the low-energy tail of the photopeak. These complex secondary events result in a net photon build-up inside the sample material. This photon build-up is a function of thickness and atomic number of the sample and also the incident photon energy, which combine to determine the intensity and spectrum of secondary photons seen by the detector in addition to primary photons. Since the multiple scattering effects are corrected, and also an optimal count rate and counting time as well as a detector of good resolution were employed, it is expected that the effects of photon build-up are negligible in the present study.

The photon build-up effects were kept to a minimum by choosing optimum count rate and the counting time. The photon build-up depends on the atomic number and the sample thickness and also on the incident photon energy. It is also a consequence of the multiple scattering occurring inside the sample. Since multiple scattering effects have been corrected and a detector of good resolution was used with optimum values of count rate and counting time, it is expected that the effects of photon build-up were negligible in the present study.

(e) *Dead time of the counting set-up*: The dead time of the multichannel analyser is a combination of the rise time of the pulse, the conversion time in the analog-to-digital converter and the data processing time. In the multichannel analyser used in the present study, there was a built-in provision for dead time correction. The percentage data correction was always <2% in the present study.

(f) *Pulse pile up effects*: The pulse pile up effects were kept to a minimum by selecting an optimum count rate and counting time, as discussed earlier.

Using the mass attenuation coefficients listed in table 1, the mean values of the atomic cross-sections, also called the effective atomic cross-sections σ_{a} in barn per atom were determined by the relation

$$\sigma_{\mathrm{a}} = \frac{M}{0.60225\sum_i n_i}\left(\frac{\mu}{\rho}\right)_c, \tag{8}$$

where $M = \sum n_i A_i$ is the molecular weight of the compound, n_i is the total number of atoms of the ith element in the molecule and A_i is the atomic mass of the ith element in a molecule. These values are listed in table 2.

5. Estimation of effective atomic number and electron density

The effective atomic number for each sample was determined by using the effective atomic cross-section σ_a. In this method, the effective atomic number of the sample was simply taken to be the value of the atomic number of an element whose σ_a matched with that of the sample in a given energy range. Clearly, this method requires a large pool of the elemental cross-section data over a wide range of energies. For this purpose, data for 38 elements in the atomic number range 1 to 83 measured earlier in this laboratory at the energies 279.2, 320.07, 514.0, 661.6, 1115.5, 1173.2 and 1332.5 keV were used [22–25]. The elemental cross-sections show a non-linear variation with respect to photon energy E and atomic number Z. Therefore, we can assume that the relation for σ could be of the type

$$\sigma = A(Z)E^{B(Z)}, \tag{9}$$

where $A(Z)$ and $B(Z)$ are constants with respect to energy and vary with atomic number. Equation (9) can be further written as

$$\ln \sigma = \ln A(Z) + B(Z) \ln E \tag{10}$$

and it represents a straight line with slope $B(Z)$ and intercept $\ln A(Z)$.

For presentation of results, the photon energy region of interest was divided into three, viz., (a) 279.2 to 320.07 keV, (b) 514.0 to 661.6 keV and (c) 1115.5 to 1332.5 keV. Within each of these regions, the values of $\ln \sigma$ were found to vary linearly with $\ln E$. So, a logarithmic regression analysis was performed between $\ln \sigma$ and $\ln E$ in all the three energy regions and the best-fit values of the slope $B(Z)$ and the intercept $\ln A(Z)$ were determined. Further, we assume that the values of $\ln A(Z)$ and $B(Z)$ are simple functions of atomic number and are given by the relations

$$\ln A(Z) = \ln A_1 + B_1 \ln Z \tag{11}$$

and

$$B(Z) = \ln A_2 + B_2 \ln Z. \tag{12}$$

Equations (11) and (12) represent straight lines with slopes B_1 and B_2 and corresponding intercepts $\ln A_1$ and $\ln A_2$ respectively. In the first two energy regions, the range of elements is divided into three groups whereas in the last energy region, it is divided into two groups as is shown in table 3. This ensures the linearity in the selected region so that the best-fit values of $\ln A_1, B_1, \ln A_2$ and B_2 could be obtained for the E and Z region of interest. These values are shown in table 3. Using these best-fit values further, we obtained the formula for Z_{eff} of the form

Table 4. Effective atomic numbers, Z_{eff}, of some TLD compounds for photon.

Compound	Photon energy (keV)						
	279.2	320.07	514.0	661.6	1115.5	1173.2	1332.5
LiF	5.979 ± 0.178	5.931 ± 0.176	5.987 ± 0.180	5.988 ± 0.178	5.973 ± 0.177	5.924 ± 0.178	5.966 ± 0.177
$CaSO_4 \cdot 2H_2O$	7.427 ± 0.221	7.377 ± 0.220	7.371 ± 0.220	7.361 ± 0.215 7.320 ± 0.146*	7.358 ± 0.216	7.374 ± 0.216	7.320 ± 0.215
$CaCO_3$	10.062 ± 0.301	10.015 ± 0.300	10.111 ± 0.302	10.052 ± 0.302	10.010 ± 0.300	10.025 ± 0.301	10.042 ± 0.300
$C_4H_6BaO_4$	12.511 ± 0.373	11.450 ± 0.342	9.382 ± 0.280	8.928 ± 0.261 8.908 ± 0.178*	8.173 ± 0.243	8.266 ± 0.247	8.163 ± 0.244
$3CdSO_4 \cdot 8H_2O$	11.360 ± 0.340	10.780 ± 0.322	9.654 ± 0.290	9.383 ± 0.275 8.824 ± 0.176*	8.950 ± 0.267	9.033 ± 0.271	8.914 ± 0.266
$CaSO_4$	11.404 ± 0.341	11.374 ± 0.341	11.316 ± 0.338	11.275 ± 0.337	11.311 ± 0.339	11.344 ± 0.340	11.351 ± 0.340
$SrSO_4$	15.668 ± 0.470	15.309 ± 0.458	15.423 ± 0.462	14.971 ± 0.439 15.187 ± 0.303*	14.442 ± 0.432	14.509 ± 0.435	14.508 ± 0.434
$CdSO_4$	19.985 ± 0.600	19.027 ± 0.571	17.274 ± 0.516	16.683 ± 0.500	16.270 ± 0.487	16.441 ± 0.493	16.349 ± 0.490
$BaSO_4$	25.221 ± 0.756	23.493 ± 0.703	19.116 ± 0.571	18.371 ± 0.545 19.118 ± 0.382*	17.923 ± 0.535	18.026 ± 0.540	17.975 ± 0.538

Values from ref. [10] (marked by *) are shown for comparison.

Table 5. Effective electron density, N_{el} (10^{23} electrons/g) measured for some TLD compounds.

Compound	Photon energy (keV)						
	279.2	320.07	514.0	661.6	1115.5	1173.2	1332.5
LiF	2.778 ± 0.083	2.756 ± 0.082	2.780 ± 0.082	2.781 ± 0.083	2.774 ± 0.081	2.751 ± 0.082	2.771 ± 0.081
$CaSO_4{\cdot}2H_2O$	3.113 ± 0.093	3.091 ± 0.091	3.089 ± 0.093	3.085 ± 0.093	3.084 ± 0.090	3.091 ± 0.093	3.068 ± 0.092
$CaCO_3$	3.027 ± 0.091	3.013 ± 0.090	3.047 ± 0.090	3.024 ± 0.089	3.012 ± 0.090	3.016 ± 0.089	3.021 ± 0.088
$C_4H_6BaO_4$	4.425 ± 0.132	4.097 ± 0.121	3.318 ± 0.099	3.157 ± 0.093	2.906 ± 0.086	2.923 ± 0.088	2.887 ± 0.086
$3CdSO_4{\cdot}8H_2O$	3.734 ± 0.111	3.543 ± 0.105	3.173 ± 0.095	3.084 ± 0.092	2.942 ± 0.085	2.969 ± 0.088	2.930 ± 0.087
$CaSO_4$	3.027 ± 0.090	3.019 ± 0.091	3.004 ± 0.090	2.993 ± 0.089	3.008 ± 0.088	3.011 ± 0.089	3.013 ± 0.087
$SrSO_4$	3.084 ± 0.091	3.012 ± 0.089	3.034 ± 0.090	2.945 ± 0.087	2.841 ± 0.085	2.854 ± 0.084	2.854 ± 0.086
$CdSO_4$	3.464 ± 0.103	3.298 ± 0.099	2.994 ± 0.090	2.892 ± 0.085	2.820 ± 0.085	2.849 ± 0.083	2.833 ± 0.084
$BaSO_4$	3.905 ± 0.115	3.637 ± 0.109	2.960 ± 0.087	2.845 ± 0.085	2.775 ± 0.082	2.791 ± 0.084	2.783 ± 0.083

$$Z_{\text{eff}} = \left[\frac{\sigma_{\text{a}}}{A_1 E^{\ln A_2}}\right]^{1/d} \tag{13}$$

where $d = B_1 + B_2 \ln E$ and E is the photon energy expressed in keV.

In obtaining this formula, we have assumed the equivalence between Z_{eff} of the sample and the Z of the equivalent element as discussed earlier.

Using the so-calculated Z_{eff} the effective electron density was calculated using the relation

$$N_{\text{el}} = \frac{Z_{\text{eff}}}{M} N_{\text{A}} \sum_i n_i. \tag{14}$$

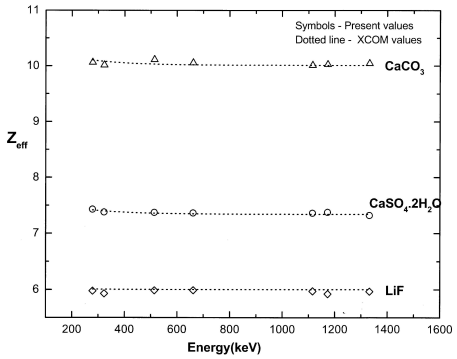

Figure 1. Variation of effective atomic number Z_{eff} with energy for $CaCO_3$, $CaSO_4{\cdot}2H_2O$ and LIF.

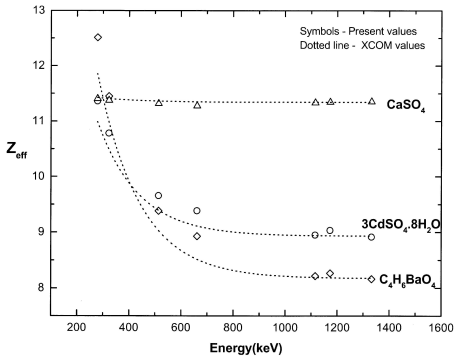

Figure 2. Variation of effective atomic number Z_{eff} with energy for $CaSO_4$, $3CdSO_4{\cdot}8H_2O$ and $C_4H_6BaO_4$.

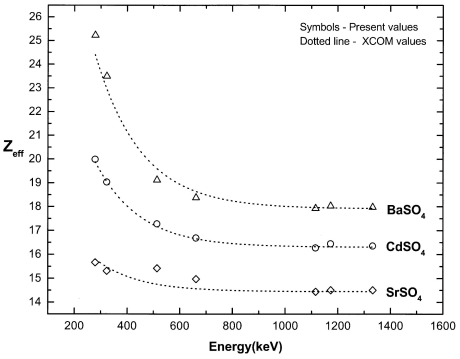

Figure 3. Variation of effective atomic number Z_{eff} with energy for $BaSO_4$, $CdSO_4$ and $SrSO_4$.

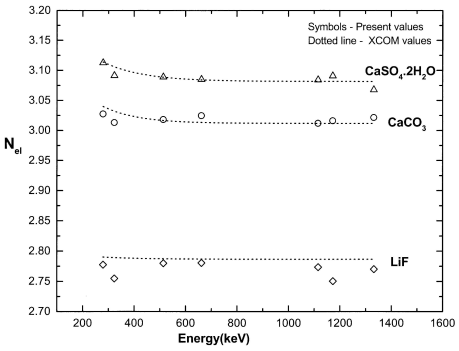

Figure 4. Variation of effective electron number N_{el} with energy for $CaSO_4{\cdot}2H_2O$, $CaCO_3$ and LiF.

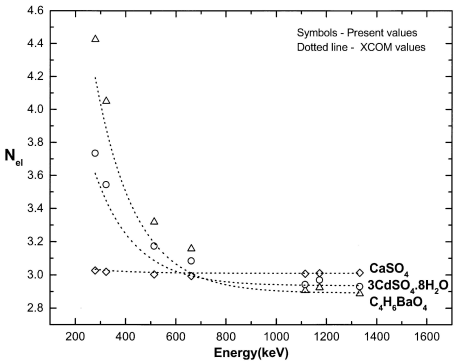

Figure 5. Variation of effective electron number N_{el} with energy for $CaSO_4$, $3CdSO_4{\cdot}8H_2O$ and $C_4H_6BaO_4$.

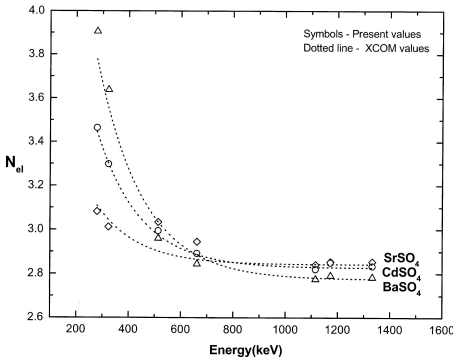

Figure 6. Variation of effective electron number N_{el} with energy for $BaSO_4$, $CdSO_4$ and $SrSO_4$.

The values of Z_{eff} and N_{el} are listed in tables 4 and 5 and compared with the other available experimental data. Plots of the present values of Z_{eff} and N_{el} vs. energy are also shown in figures 1–6 along with the XCOM values [21].

6. Conclusions

In the present work, the Z_{eff} values and the electron densities of the TLD compounds were obtained using the measured values of their mass attenuation coefficients in the photon energy range 200 to 1500 keV. The values of effective atomic numbers and the electron densities of TLD compounds are in agreement with the other available data at energies of interest. To our knowledge, the data presented are the first of their kind and have not been reported earlier.

References

[1] C M Davisson and R D Evans, *Phys. Rev.* **81**, 104 (1951)
[2] A L Conner, H F Atwater, E H Plassman and J H McCray, *Phys. Rev.* **A1**, 539 (1977)
[3] B Goswami and N Chaudhuri, *Phys. Rev.* **A7**, 1912 (1973)
[4] A H El-Kateb, A H Hassan and A S Abdul Hamid, *1st Egyptian-British Conf. on Biophysics* (Cairo University, 1987) p. 442
[5] A H El-Kateb, A H Hassan, S A El-Hennawi and A S Abdul Hamid, *Nucl. Sci. J.* **26**, 133 (1989)
[6] A H El-Kateb and A S Abdul Hamid, *Int. J. Appl. Radiat. Isotopes* **42**, 303 (1991)
[7] D A Bradley, C S Chong and A M Ghose, *Int. J. Appl. Radiat. Isotopes* **36**, 743 (1985)
[8] D A Bradley, C S Chong and A M Ghose, *Int. J. Appl. Radiat. Isotopes* **37**, 1195 (1986)
[9] A Perumallu, A S Nageswara Rao and G Krishna Rao, *Physica* **C132**, 388 (1985)
[10] Shivaramu, R Amutha and V Ramprasath, *Nucl. Sci. Eng.* **132**, 148 (1999)
[11] Shivaramu and V Ramprasath, *Nucl. Instrum. Methods* **B168**, 294 (2000)

[12] D F Jackson and D J Hawkes, *Phys. Rev.* **70**, 169 (1981)
[13] G J Hine, *Phys. Rev.* **85**, 725 (1952)
[14] K Parthasaradhi, *Ind. J. Pure Appl. Phys.* **6**, 609 (1968)
[15] D V Krishna Reddy, K Suresh Babu and S Chandra Lingam, *Can. J. Phys.* **63**, 1421 (1985)
[16] A Perumallu, A S Nageshwara Rao and G Krishna Rao, *Can. J. Phys.* **62**, 454 (1984)
[17] S Chandra Lingam, K Suresh Babu and D V Krishna Reddy, *Indian J. Phys.* **A53**, 285 (1984)
[18] K Singh, Rajinderjit Kumar, Vandana and Vijay Kumar, *Radiat. Phys. Chem.* **47**, 535 (1995)
[19] H P Schatzler, *Int. J. Appl. Radiat. Isotopes* **30**, 115 (1979)
[20] J H Hubbell and S M Seltzer, Report, NISTIR-5632 (1995)
[21] M J Berger and J H Hubbell, Report, NBSIR 87, *XCOM: Photon cross sections on a personal computer* (1987) p. 3597
[22] T K Umesh, C Ranganathaiah, Ramakrishna Gowda, K S Puttaswamy and B Sanjeevaiah, *Phys. Rev.* **A23**, 2365 (1981)
[23] T K Umesh, C Ranganathaiah and B Sanjeevaiah, *Phys. Rev.* **A29**, 387 (1984)
[24] T K Umesh, Ramakrishna Gowda and B Sanjeevaiah, *Phys. Rev.* **A25**, 1986 (1981)
[25] T K Umesh, S J Anasuya, J Shylaja Kumari, Channegowda, K P Gopinathan Nair and Ramakrishna Gowda, *Phys. Rev.* **A45**, 2101 (1992)
[26] R D Deslattes, *Acta Crystallogr.* **A25**, 89 (1969)
[27] J H Hubbell and M J Berger, Photon attenuation in: *Engineering compendium on radiation shielding* edited by R G Jaerger (IAEA, Vienna, Austria, 1968) vol. 1, ch. 4, p. 198
[28] R W Carter, R H Rohrer, W H Carlton and G R Dyer, *Health Phys.* **13**, 593 (1967)